Characterization of Formed TRIP1180 Steel Sheet Surface After Stamping with PVD-Coated Tools

Junho Bang[1] · Gihyun Bae[1] · Minki Kim[1] · Junghan Song[1] · Myoung-Gyu Lee[2] · Hong-Gee Kim[3]

© The Author(s) 2023

Abstract

The wear tests are conducted on bending punches deposited with PVD CrN and AlTiCrN coatings using the newly proposed progressive die. Then, the surface quality of the formed product is characterized through the surface roughness measurement after forming of TRIP1180 steel sheets. The correlation between the tool wear, in terms of wear depth and roughness and the product surface roughness can be quantitatively analyzed. The results show that the roughness remains comparable to that of the as-received surface before failure occurs, which represents smooth product surface without severe scratches and defects. While micro scratches on the punch surface have no effect on the quality of the product surface, severe fretting wear on the punch surface leads to a deterioration in the surface quality. Once initiated in the stamping process, the wear progresses exponentially within short time. The wear is also characterized as less than the coating thickness, but it results in complete removal of the coating layer. The partially worn punch plows the product surface, causing surface scratches with grooves and ridges, resulting in the roughness of 1.0 µm. In contrast, the surface with completely damaged coatings is extremely rough, with the roughness of 2.0 µm. This study presents the efficient method to evaluate the tool wear progression by indirectly measuring the product surface quality with reliably high precision.

Keywords Ultra-high-strength steel · Wear · PVD coating · Cold stamping process · Progressive die

Abbreviations

CLSM   Confocal laser scanning microscopy
PVD   Physical vapor deposition
TRIP   Transformation induced plasticity

1 Introduction

With the increasing demand for eco-friendly vehicles such as battery-powered and hydrogen-powered electric vehicles, in the recent automobile industry, there has been a growing demand for reducing vehicle weight. Efficient lightweighting of automobile bodies is achieved through substitution of traditional materials with lightweight alternatives, including advanced high-strength steels (AHSS), aluminum alloys, magnesium alloys, carbon-fiber-reinforced composites, and glass fiber composites. Among these lightweight materials, AHSS is the most economical for manufacturing automotive body parts, despite providing the least weight reduction [1–3]. Sun et al. [4] evaluated the global warming potential per kg of AHSS, Al alloy, and carbon-fiber-reinforced plastic and concluded that AHSS has the lowest carbon dioxide emissions. Additionally, Safari et al. [5] conducted simulations of full frontal impact, side-impact, and roof crush tests, which showed that AHSS materials exhibit superior crash safety performance. For these reasons, average usage of AHSS in vehicle automobile bodies has significantly increased in recent years due to its high strength-to-weight ratio, improved crash performance, and reduced environmental impact [6]. Due to the low uniform elongation and high tensile strength of AHSS sheets, they can lead to problems such as limited formability, high springback, and premature tool wear. The forming of AHSS sheets is generally accompanied by higher contact pressure on the tool surface, resulting in a vulnerability to tool wear and premature wear.

✉ Junghan Song
   jhsong@kitech.re.kr

1   Molding & Metal Forming R&D Department, Korea Institute of Industrial Technology (KITECH), Incheon 21999, Republic of Korea

2   Department of Materials Science and Engineering, Seoul National University & RIAM, Seoul 08826, Republic of Korea

3   Materials Forming Research Group, POSCO Global R&D Center, Incheon 21985, Republic of Korea

Because automotive metallic components are typically mass-produced, the cold forming process is preferred to reduce manufacturing costs, but it also increases the vulnerability of the tools to wear. The tool wear can cause various problems such as reduced productivity, increased maintenance costs, and decreased product surface quality. Therefore, effective tool wear management is an essential consideration to prevent these problems and ensure an efficient mass production process.

The continuous increase in the application of AHSS sheets in automobile body has led to various issues related to the tool wear. Numerous studies have been conducted to characterize the wear behavior and extend the lifespan of the tools. Surface roughness and machining errors of the tool are particularly susceptible to galling and significantly impact the tool's wear lifespan during the sheet metal forming process [7–9]. By appropriately polishing the tool surface to eliminate any irregularities and asperities that can initiate material transfer, the tendency for galling can be significantly reduced, leading to a considerably prolonged tool lifespan, both in lubricated and unlubricated tool conditions [10–12]. Coating techniques are another potential approach for extending the wear lifespan. Wear characteristics and resistance of various coatings have been evaluated and compared in the sheet metal forming [13–15]. Moreover, the choice of the tool materials plays a crucial role in improving wear resistance in the sheet metal forming process. Büyükkayacı et al. [16] confirmed the effect of mechanical alloying times on the wear performance of the Fe–Cu–C alloy produced through the Powder Metallurgy method. Sıralı et al. [17] investigated the impact of grain size reduction with respect to the addition amount of Ti on the microstructure, hardness, and wear behavior of the titanium–zirconium–molybdenum alloys. Ogunbiyi et al. [18] substantiated that the addition of grapheme nanoplatelets into Inconel 738 low carbon composites using the spark plasma sintering technique enhances wear resistance. Groche and Christiany [19] investigated the wear characteristics and development of different tool materials using a strip drawing test. The wear resistance of tool materials can be improved by controlling various heat treatment parameters. Gonzalez-Pociño et al. [20] investigated the adhesive wear resistance of tool steel by intentionally modifying quenching, tempering, and nitriding processes and proposed optimal heat treatment parameters to enhance the adhesive wear resistance in sheet metal forming. Woodward et al. [21] studied the sliding wear behavior of G320 grey cast iron under various microstructure conditions induced by quenching and tempering heat treatments. Jeong and Shim [22] utilized FeCrMoVW powder, a powder-metallurgy-based tool steel, to coat an AlSI D2 substrate using additive manufacturing. The deposited layers exhibited a hardness approximately 20% higher than QT-D2 (56HRc), attributed to the presence

of fine grains within the deposited regions. Additionally, the as-built FeCrMoVW showed improved wear resistance and compressive strength compared to QT-D2. Jeyaprakash et al. [23] investigated Inconel-625 superalloy produced through Selective Laser Melting (SLM) process. The specimen manufactured by SLM demonstrated enhanced nano-hardness and wear resistance attributed to the formation of angular columnar cell, fine hard phases, effective nodding strength and defect-free surface.

The aforementioned papers suggested that the wear resistance of a tool can be enhanced by managing various tooling and process parameters that impact its wear performance. This effective management can delay the onset of tool wear and reduce maintenance costs in the stamping process. However, these studies have limitations in predicting the evolutionary wear behavior of the tool and the initiation of the tool failure, which can lead to decreased productivity due to unplanned machine downtime. To address this, Bang et al. [24] proposed a power-law-type wear prediction model based on Pin-on-disk tests and the Taguchi method to predict the wear of CrN-coated tools in the stamping process of advanced high-strength steel sheets. In order to predict and evaluate the evolutionary behavior of tool wear in the stamping process, Bang et al. [25] suggested the wear measurement methods such as wear depth and roughness measurement, as well as surface imaging. However, measuring the wear amount of large-volume tools in the stamping process of automotive components is challenging and can result in decreased productivity due to machine downtime. While the studies mentioned above have focused on the perspective of the tools for efficient process management, it is important to note that the tool wear occurs when tool comes into contact with the product surface during sheet metal stamping, directly affecting the product surface quality. Cumulative relative motion between the tool and product leads to deterioration in product surface quality. Therefore, by quantitatively evaluating product surface quality and analyzing its correlation with tool wear state, it becomes possible to predict tool wear initiation based on the product surface quality. However, research on the impact of tool surface characteristics on the surface quality of products in the sheet metal forming process is virtually non-existent. Analyzing the evolutionary behavior of product surface conditions can provide guidance for tracking tool surface conditions and wear. Examining tool surface conditions during automobile mass production can result in increased machine downtime. Therefore, predicting tool wear by observing product surface quality enables efficient process management without unnecessary machine downtime. Additionally, the evolutionary quality and characteristics of the product surface can serve as evidence for real-time process monitoring using machine learning, deep learning, and computer vision techniques to detect tool wear.

Fig. 1 Experimental setup for continuous wear test [22]: **a** isometric view of schematics; **b** top view of schematics; **c** progressive die set; **d** steel strip

(a)

(b)

(c)

(d)
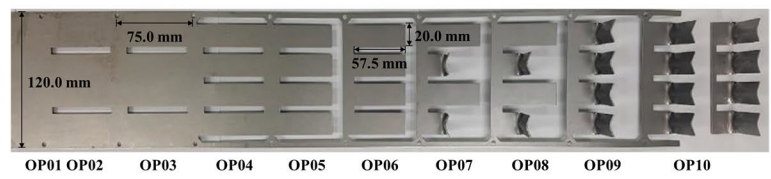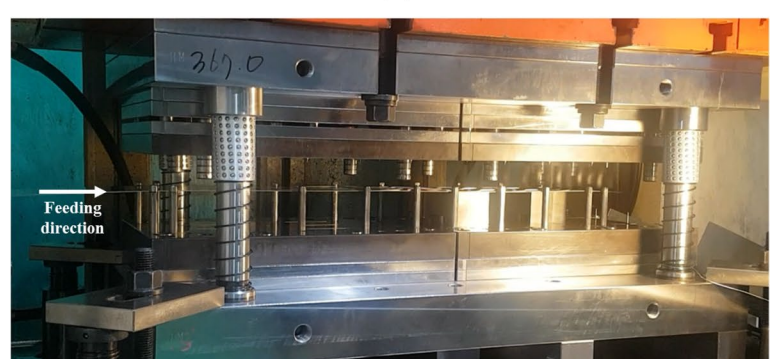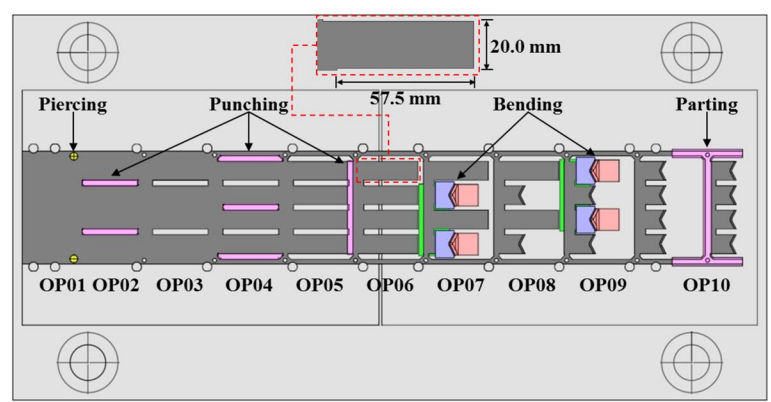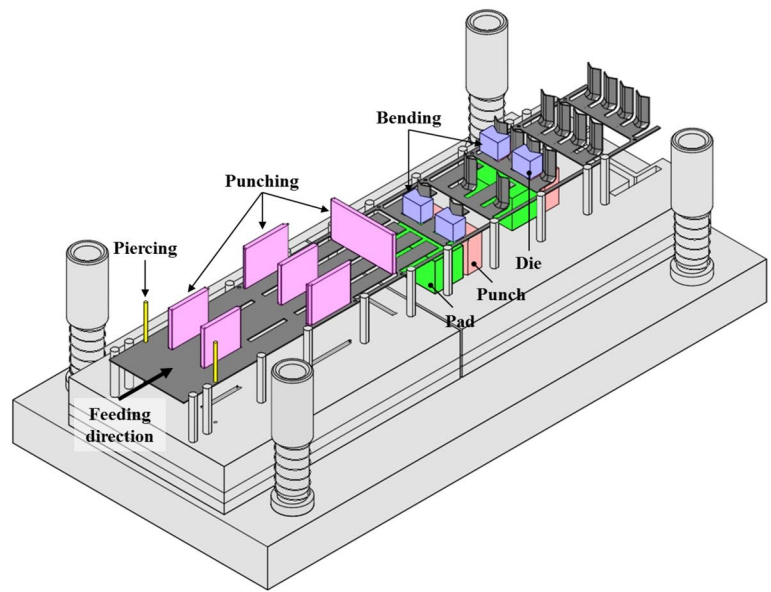
The primary objective of this paper is to examine the influence of the tool surface characteristics on the product surface quality in the forming process of TRIP1180 steel sheet using PVD-coated tool. A progressive die set was employed for the systematic and efficient wear test. The surface quality characteristics of the product formed with PVD-coated punches were quantitatively evaluated. The product surface quality was assessed by measuring roughness and capturing the surface images. Additionally, the impact of tool surface characteristics, including wear depth and roughness, on the product surface quality was investigated, and their correlation was analyzed.

2 Experimental Setup

2.1 Continuous Wear Testing Method

The tool wear test for cold sheet metal forming process requires significant time, materials, and labor. In this study, to facilitate continuous and efficient wear testing, a progressive die set was employed. The progressive die set is designed to encompass multiple metalworking operations within a single tool set. As the sheet metal progresses through each operation, it is gradually formed into the final product shape. As a result, continuous mass production of products at a constant work rate is possible.

The design of the progressive die set and the experimental apparatus were based on a previous study by Bang et al. [25]. The layout of the metalworking operations in the progressive die set is depicted in Fig. 1a, b. The design includes piercing, punching, bending, and parting operations. The piercing operation (OP1) involves creating holes in the sheet metal using a cylindrical shearing punch. The sheet metal is then supplied to the progressive die set at constant intervals of 75.0 mm through these holes. The punching operation (OP2, OP4, and OP5) utilizes rectangular shearing punches to create blank shapes with a width of 20.0 mm and a height of 57.5 mm. The bending operation (OP7, and OP9) employs a bending punch to form the blank, during which wear occurs on the punch surface. The punch stroke is designed to be 35.0 mm. By designing four types of bending punches to be processed simultaneously, the time, materials, and labor required for the wear test were reduced. The parting operation (OP10) involves cutting the completed product from the sheet metal using a shearing punch. The test was conducted at a press speed of 15 spm (strokes per minute), which is a common speed in the automotive component forming processes. Figure 1(c) shows the progressive die set installed on the mechanical press, and Fig. 1(d) illustrates a sample that was continuously formed using the progressive die set.
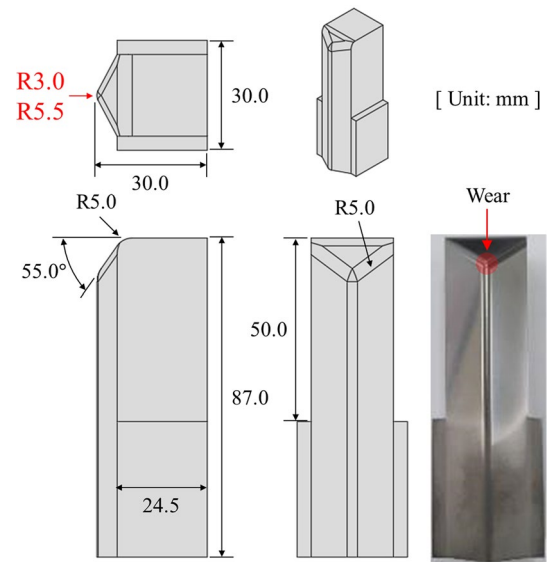

Fig. 2 Detailed design of the punch used in the wear test [22]

The progressive die set was installed in a mechanical press, and a 120 mm wide coil was fed by feeder and uncoiler to enable continuous wear testing.

2.2 Punch Design

In the sheet metal forming process, the contact pressure and sliding distance play a significant role in the tool wear life [26, 27]. Tool wear predominantly occurs in the curved area of the tool where contact pressure and sliding distance are concentrated. Smaller curvature radius results in higher contact pressure on the mold surface, making it more susceptible to wear. In this study, the shape of the tool's vulnerable area in the stamping process of automotive parts was considered when designing the punch for the wear test. The punch design was based on the previous study by Bang et al. [25]. The punch was specifically designed to concentrate contact pressure on the curved area of the punch during forming the blank, as shown in Fig. 2. The punches had two different curvature radii, 3.0 mm and 5.5 mm. The punches were made in insert type for convenient measurement of wear and easy replacement of the punch. To prevent ironing, a die-to-punch gap of 1.32 mm was designed, which corresponds to a 10% clearance considering the sheet thickness of 1.2 mm. The punch stroke was set to 35.0 mm.

2.3 Materials

In this research, TRIP1180 steel sheet with a thickness of 1.2 mm was used. The Vickers hardness of the TRIP1180 1.2t sheet was measured to be 373.2 ± 7.1 $HV_{0.1}$. The tensile

material properties of the TRIP1180 1.2t sheet are summarized in Table 1. The punches utilized in the study were made of D2 (ASTM A 681–08) tool steel produced by POSCO Pohang steelworks. The Vickers hardness of D2 was measured to be 788.5 ± 12.2 $HV_{0.1}$. The punch surface was coated with CrN and AlTiCrN using the PVD (physical vapor deposition) method. The thickness of the CrN and AlTiCrN coating layers was measured to be 13.4 ± 0.4 μm and 14.8 ± 0.9 μm, respectively. The Vickers hardness of the CrN and AlTiCrN coatings was $2,105.9 \pm 15.5$ $HV_{0.08}$ and $3,818.3 \pm 36.5$ $HV_{0.08}$, respectively. The chemical compositions of TRIP1180, and D2 are provided in Table 2.

2.4 Test Conditions

Table 3 presents the different combinations of tooling parameters for each punch. Punch 1, with a curvature radius of 5.5 mm where relatively low contact pressure is concentrated, was coated with PVD CrN with the Vickers hardness of $2,105.9 \pm 15.5$ $HV_{0.08}$. Punch 2, with a curvature radius of 3.0 mm which is more susceptible to wear, was coated with PVD AlTiCrN with a higher hardness of $3,818.3 \pm 36.5$ $HV_{0.08}$. The evolutionary wear characteristics of these two types of PVD-coated punches were evaluated in the forming process of TRIP1180 with a thickness of 1.2 mm. Furthermore, the impact of this wear on the surface quality characteristics of the resulting product was compared and evaluated.

2.5 Product Surface Characterization

To evaluate and characterize the surface quality of products formed by each punch, roughness and imaging of the product surface were examined using the Confocal laser scanning microscopy (CLSM; LEXT OLS3100 manufactured by OLYMPUS), which enables 3D imaging and surface profiling. The roughness and images were measured on the product surface in contact with the bending punch during the bending operation. As shown in the Fig. 3, measurements were taken at 5 mm intervals up to 30 mm in the

Table 3 Punches used in the wear test, manufactured with a combination of various tooling parameters [22]

	Punch radius	Coating	Punch material
Punch 1	5.5 mm (R5.5)	PVD CrN	D2
Punch 2	3.0 mm (R3.0)	PVD AlTiCrN	

stamping direction (sliding contact direction) from the bottom surface of the sheet metal. To ensure accurate roughness measurements, a $50 \times$ objective lens was used, and the size of the evaluation area was 256 μm in width and length. To remove the wave component from the primary component, a 1/3 cut-off wavelength was applied. The arithmetical mean height (Sa) was used to measure roughness. Sa represents the mean of the average height difference for the average plane, as follows:

$$Sa = \frac{1}{A} \iint\limits_{A} |Z(x,y)| dxdy \tag{1}$$

where A represents the measurement area, and Z(x,y) represents the height deviation from the average plane at each position (x,y). The surface roughness of the as-received materials was measured to be 0.582 ± 0.018 μm. The wear tests were conducted until severe scratches and defects were discovered on the product surface. To evaluate the evolutionary behavior of the product surface quality, the product was sampled at frequent intervals of 250 stamping hits.

3 Test Results and Discussion

3.1 Product Surface Conditions

The wear tests were performed with each punch, and the surface quality from the perspective of the blank in contact with the punch was quantitatively evaluated and discussed. To examine the evolution of product surface conditions, the product samples were taken at frequent intervals

Table 1 Tensile properties of a TRIP1180 (1.2 mm thickness) steel sheet

Yield stress (MPa)	Ultimate tensile stress (MPa)	Swift hardening law $\sigma = k(\varepsilon_0 + \varepsilon)^n$			R-value		
		$k(MPa)$	ε_0	n	0°	45°	90°
933	1196	1584.6	0.0036	0.086	0.738	0.979	0.867

Table 2 Chemical compositions of TRIP1180 steel sheet and D2 tool steel (wt%)

	C	Si	Mn	Cr	Mo	V	P	S
TRIP1180	0.285	1.61	2.15	–	–	–	0.018	0.001
D2	1.55	0.26	0.30	11.36	0.81	0.20	–	–

Fig. 3 Roughness measurement locations on the product surface and example images at each measurement location
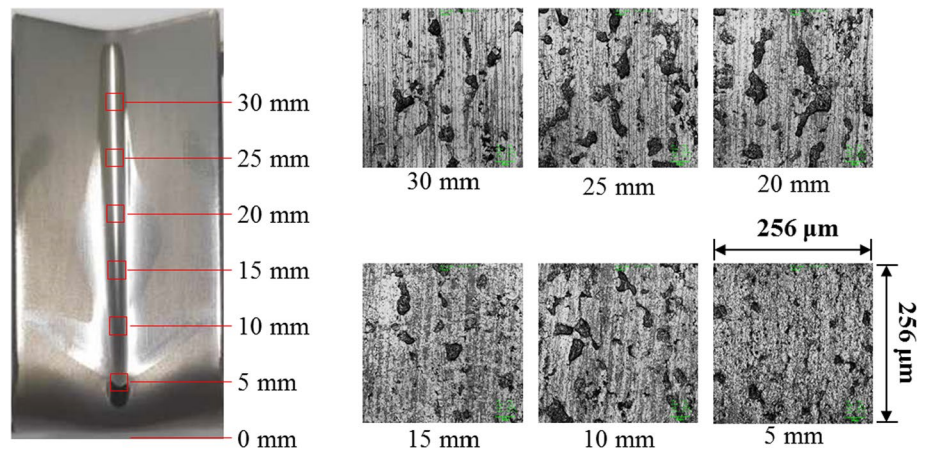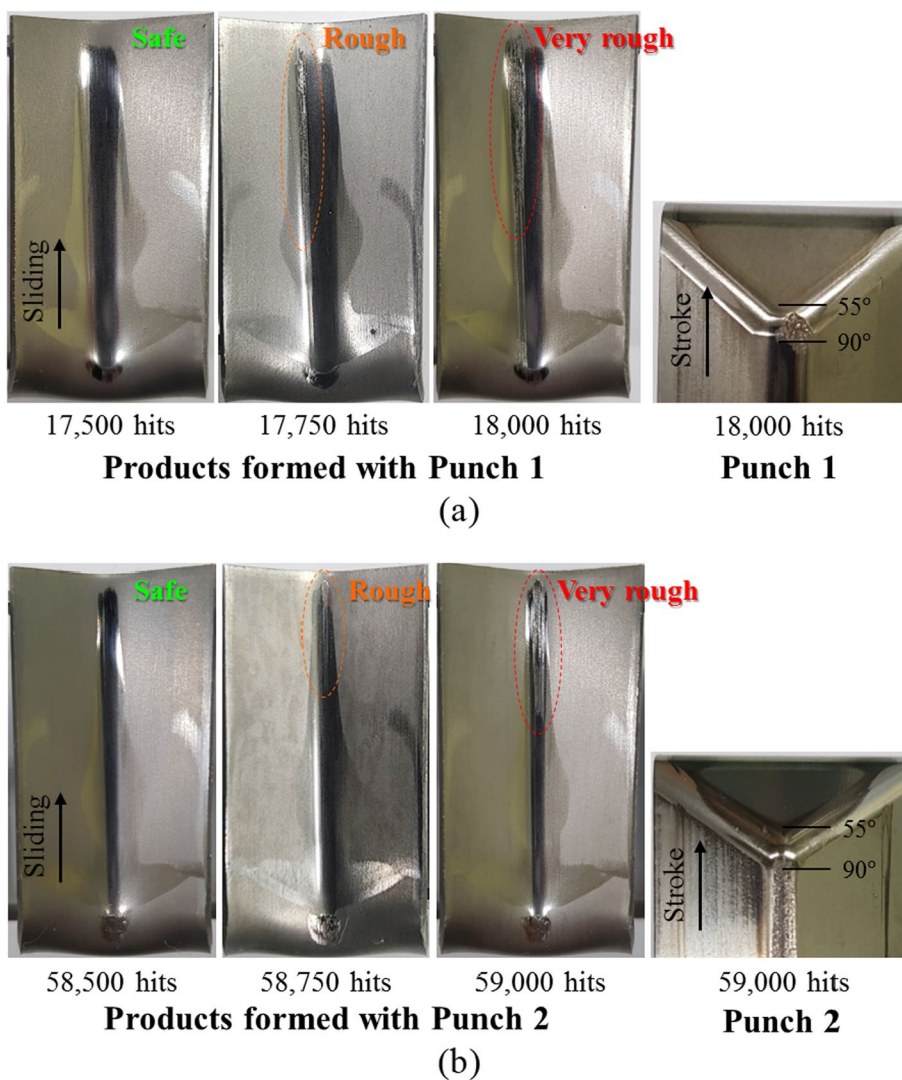

of 250 stamping hits. The wear tests continued until severe scratches and defects were visually confirmed on the product surface. Punch 1 was discontinued after 18,000 stamping hits, while Punch 2 was discontinued after 59,000 stamping hits. Figure 4 illustrates the change in the surface condition of products formed with each punch. Up to 17,500 for Punch 1 and 58,500 hits for Punch 2, the product surfaces remained smooth without any scratches and defects. After additional 250 stamping hits, minor scratches were observed on both product surfaces. However, severe defects became evident on both product surfaces after the wear tests. Figure 5 presents the roughness and images measured on the product surface formed with each bending punch. Prior to the appearance of scratches and defects for both cases, the roughness measured at each location showed similar values with respect to stamping hits and was comparable with the roughness of the as-received material (0.582 ± 0.018 μm). Moreover, the product surface images at all measurement locations appeared smooth without scratches or defects. However, after additional 250 stamping hits, scratches parallel to the sliding contact direction became noticeable in the surface images. After the wear test, the observed images exhibited very rough surfaces with severe defects. For the product formed with Punch 1 (see Fig. 5a), the images observed from 10 to 30 mm of the product surface displayed grooves and ridges parallel to the sliding contact direction, and the roughness increased to a maximum of 1.061 μm at 10 mm measurement location after 17,750 hits. After 18,000 hits (end of the wear test), extremely high roughness was measured from 10 to 30 mm from the product bottom, with a maximum roughness of 2.430 μm at 30 mm measurement location. The surface conditions at the corresponding locations exhibited extremely rough defects without grooves and ridges. For the product formed with Punch 2 (see Fig. 5b), grooves and ridges in the sliding contact direction were observed at 25 and 30 mm after 58,750 hits, and the roughness increased to a maximum of 1.061 μm at 10 mm measurement location. After 59,000 hits (end of the wear test), relatively high

roughness was measured at 25 and 30 mm from the product bottom, with a maximum roughness of 1.983 μm at 30 mm measurement location. Extremely severe defects without grooves and ridges were observed at these locations.

In Fig. 5, it can be observed that before the appearance of scratches and defects on the product surface, the roughness measured at 5 mm measurement location is higher compared to the roughness observed at the 30 mm measurement location. Furthermore, the roughness gradually decreases toward 30 mm measurement location. This phenomenon can be explained by examining the contact pressure response over the punch radius, as predicted by Bang et al. [28], shown in Fig. 6. Figure 6a illustrates the contact pressure distribution over the punch radius for the punches with a curvature radii of 3.0 mm and 5.5 mmm and the corresponding contact locations on the product surface. Figure 6b shows the maximum contact pressure over the punch radius with respect to the progression of the punch stroke. During bending process, the blank initially contacts 55° of the punch radius and then wraps around the punch radius up to 88°. This region corresponds to a punch stroke of approximately 10 mm to 13 mm, experiencing a relatively high contact pressure with maximum values of 1.707 GPa and 1.372 GPa for curvature radii of 3.0 mm and 5.5 mm, respectively (see Fig. 6). Consequently, the 5 mm measurement location on the product exhibits relatively high roughness due to the relatively high contact pressure within the punch stroke range of approximately 10 mm to 13 mm. In the punch stroke range between approximately 13 mm and 35 mm, the blank maintains steady contact with the punch radius around 67.3° and 72.9° for curvature radii of 3.0 mm and 5.5 mm, respectively (see Fig. 6a), resulting in relatively low contact pressure (see Fig. 6b). Because this punch stroke range contacts 10 mm to 30 mm measurement locations of the product, relatively low roughness is measured. As shown in Fig. 6b, Punch 1 (with a curvature radius of 5.5 mm) experiences lower contact pressure compared to Punch 2 (with a curvature radius of 3.0 mm). Therefore, the surface roughness of the product

Fig. 4 Change in product surface quality and surface condition of worn punches after the wear test: **a** Punch 1; **b** Punch 2


Safe   Rough   Very rough

Sliding

Stroke   55°   90°

17,500 hits   17,750 hits   18,000 hits   18,000 hits

Products formed with Punch 1   **Punch 1**

(a)

Safe   Rough   Very rough

Sliding

Stroke   55°   90°

58,500 hits   58,750 hits   59,000 hits   59,000 hits

Products formed with Punch 2   **Punch 2**

(b)

formed by Punch 2 is approximately 0.15 μm higher than that of Punch 1 (see Fig. 5).

3.2 Evolutionary Behaviors of Product Surface Quality in Relation to Stamping Hits

The punch surface condition deteriorates due to cumulative relative motion with the blank, which affects the surface quality of the product. In order to analyze the evolutionary behavior of the product surface quality in relation to the change of the punch surface condition, the surface imaging and roughness of the punches were examined in relation to stamping hits. However, due to the difficulty of inspecting the surface condition of the punches in a frequent measuring cycle, the surface imaging and roughness of Punch 1 were examined prior to wear test (as-produced), and after 5000, and 10,000 stamping hits, as well as after 18,000 stamping hits (after failure), as shown in Fig. 7a, b. A detailed explanation of examining the surface condition of Punch 1 was

based on the previous study by Bang et al. [25]. To confirm the effect of the wear depth of Punch 1 on the product surface quality, the experimental results of wear depth for the same punch were referred to from the study by Bang et al. [25], as shown in Fig. 7c. Additionally, Fig. 8 illustrates the surface images, roughness, and wear depth of Punch 2 with respect to the number of stamping hits, which were referenced from a previous study conducted by Bang et al. [25].

The as-produced surface of Punch 1 appeared smooth without any scratches or defects, with an average roughness of approximately 0.226 μm. After 5000 and 10,000 stamping hits, micro scratches were observed throughout the observation area of the punch surface, resulting in an increase in the measured roughness by approximately 0.03 μm on average compared to that of the as-produced condition. However, no significant the wear depth was observed in all measurement areas, and the formed product surface was not rough (see Fig. 5a). Therefore, it was confirmed that the micro scratches on the punch surface did not contribute to the deterioration

(a)

(b)
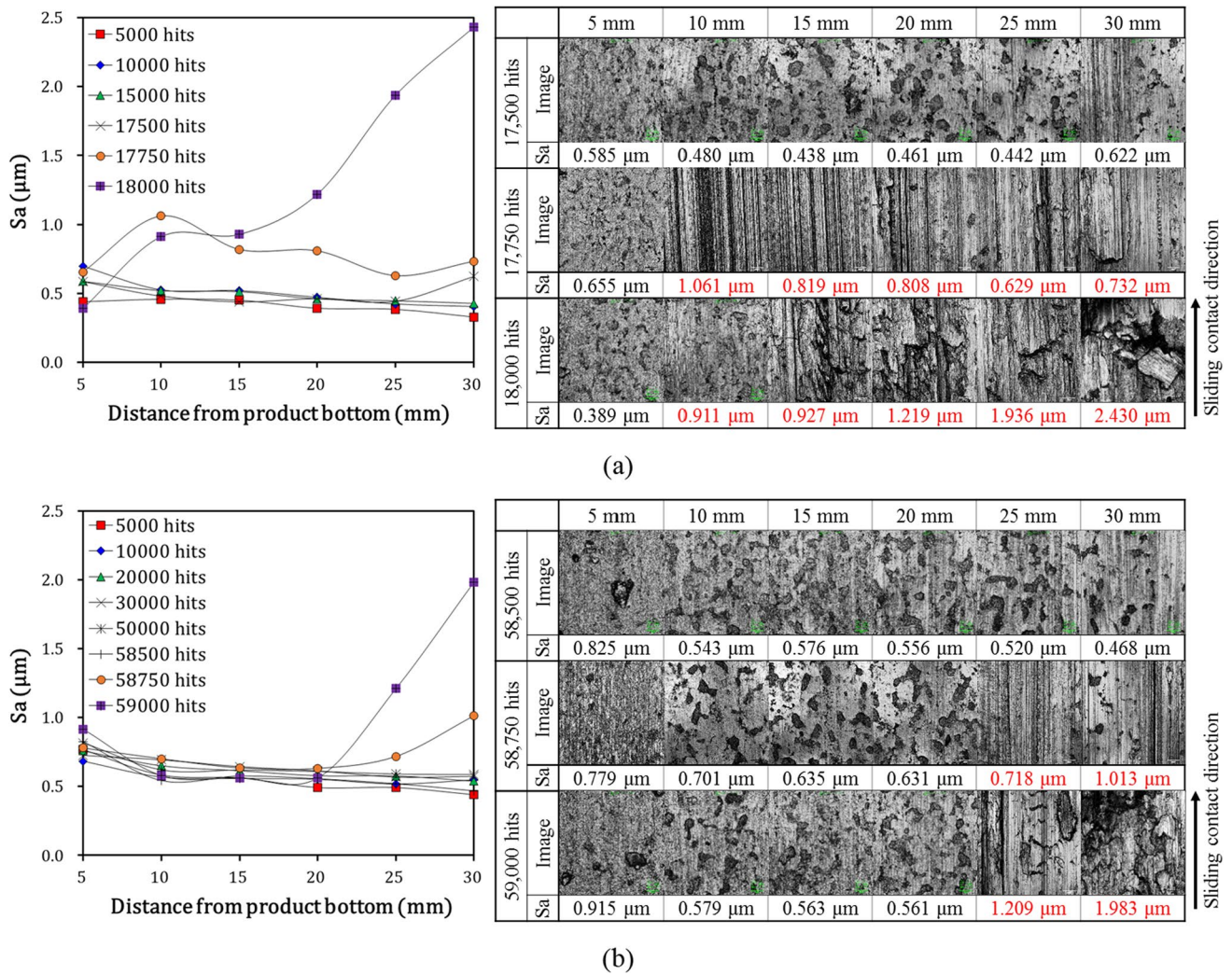
Fig. 5 Roughness and images measured on the product surface formed with: **a** Punch 1; **b** Punch 2

of the product surface quality. After 18,000 stamping hits (after failure), severe wear occurred on punch radius from 76° to 90°, resulting in significantly high roughness, with a maximum roughness of 1.668 μm at 82°. The range of the severe wear track was consistent with that of the wear depth results, with a maximum wear depth of 15.7 μm at 87°. After 18,000 stamping hits, the product surface formed by the worn Punch 1 exhibited a very rough surface, with a maximum roughness of 2.43 μm. The wear test results for Punch 2 showed a same tendency to Punch 1. The as-produced surface of Punch 2 had an average roughness of approximately 0.232 μm, and no scratches or defects were observed. Up to 50,000 stamping hits, the micro scratches occurred on the punch surface, resulting in an increase of approximately 0.15 μm in the punch roughness. However, no significant change in the wear depth was observed, and the surface of the formed product remained smooth without any scratches or defects (see Fig. 5b). After 59,000 stamping, the

severe wear was observed on the punch radius from 78° to 90°, with a maximum roughness and wear depth of 1.106 and 17.4 μm, respectively, at 88° on the punch radius. The product formed by the worn Punch 2 exhibited a very rough surface, with a maximum roughness of 2.43 μm (Fig. 5b).

Figure 9 illustrates the relationship between the punch surface condition and the product surface quality with respect to the number of stamping hits. The red quadrangle marks indicate the wear depth of the punch, while the blue rhombus and circle marks indicate the change in roughness (ΔSa) relative to the initial conditions of the punch and products, respectively. Prior to the occurrence of severe wear on the surface of Punch 1 (at 5000 and 10,000 stamping hits), the punch roughness slightly increased by approximately 0.03 μm compared to that of the as-produced, due to the micro scratches. These micro scratches had little effect on the change of the wear depth on the punch radius, and resulted in an increase of approximately 0.10 μm in
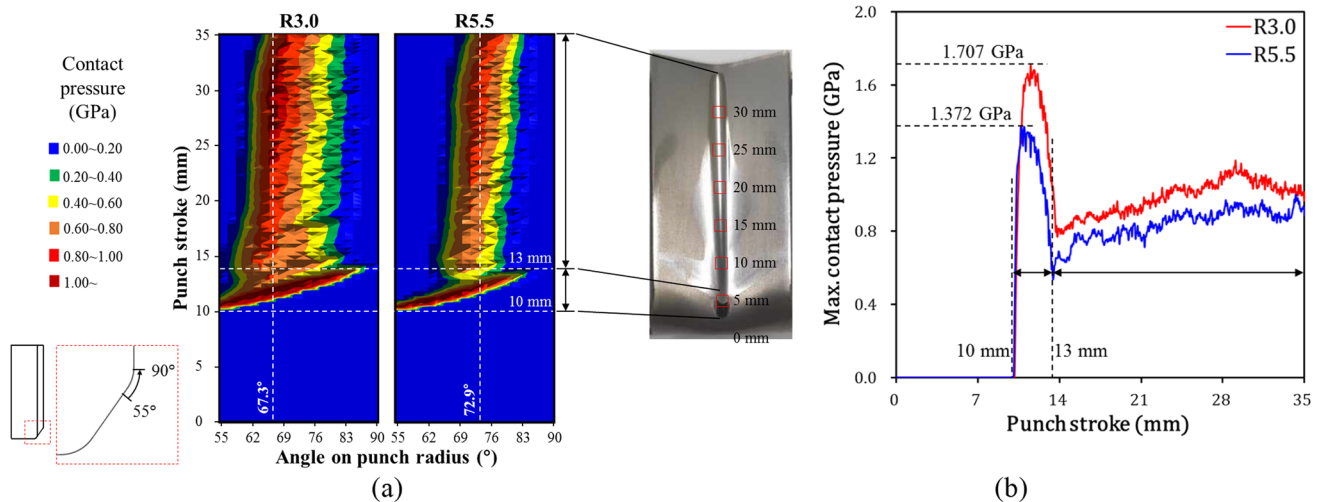
Fig. 6 Evolutionary contact pressure responses over the punch radius with a curvature radius of 3.0 mm and 5.5 mm: **a** Contact pressure distribution over punch radius and corresponding contact location on the product surface; **b** Maximum contact pressure over the punch radius with respect to the progression of the punch stroke [25]

product roughness. However, they did not visually degrade the product surface quality. When severe wear occurred on the punch radius at 18,000 stamping hits, the wear depth reached 15.7 μm, indicating complete wear-off of the CrN coating layer (13.4 ± 0.4 μm), and the punch roughness significantly increased by 1.411 μm. As the punch surface condition directly affects the product surface quality, the product roughness also deteriorated significantly, increasing by 2.022 μm. The evolutionary wear behaviors of Punch 2 also exhibited a similar tendency to Punch 1. Prior to failure (up to 50,000 stamping hits), the punch roughness and wear depth experienced minor changes due to the micro scratches, which had a limited impact on the product surface quality. However, after 59,000 stamping hits, severe wear occurred on the punch surface, with a maximum wear depth of 17.4 μm, indicating complete wear-out of the AlTiCrN coating layer (14.8 ± 0.4 μm). The measured punch roughness also increased significantly by 0.801 μm. Consequently, the product roughness reached 1.983 μm, indicating a significant deterioration in surface quality.

Based on the experimental results, it is evident that the product surface quality is directly influenced by the tool surface condition, and conversely, the tool surface condition can be inferred from the product surface quality. Figure 10 illustrates this relationship. In the case of the product formed by Punch 1, it can be observed that the roughness change (ΔSa) after 17,750 stamping hits was 0.653 μm. This value exponentially increased to 2.022 μm after 18,000 stamping hits. Similarly, for the product formed by Punch 2, the roughness change (ΔSa) was 0.457 μm after 58,750 stamping hits, and it exponentially increased to 1.427 μm after 59,000 stamping hits. Both punches exhibited an exponential

increase in product roughness during last 500 stamping hits (see Fig. 10). This suggests that that after reaching the failure point, both punches experienced similar wear mechanisms and underwent wear evolution at a comparable rate. The detailed discussion of the tool wear mechanisms will be covered in the subsequent chapter.

In the mass production process of automotive body parts, tool wear can cause the problems such as decreased productivity, increased tool maintenance costs, and decreased product quality. Therefore, efficient management of tools is crucial in process management. However, real-time examination of tool wear during the mass production process can temporarily halt the process, leading to decreased productivity. Experimental results showed that in the forming process of TRIP1180 steel sheet using PVD-coated tools, the tool surface condition with respect to stamping hits is consistent with the product surface quality, and the product surface quality accurately reflects the wear state of the tool. Premature replacement of tools before reaching their wear lifetime can result in increased tool maintenance costs and decreased productivity. Hence, efficient and economical tool management in the mass production process of automotive body parts can be achieved through careful observation of the product surface quality in order to detect the tool wear.

3.3 Wear Mechanism

Figure 11 illustrates the 3D structures of the surfaces observed at 30 mm from the bottom of the product formed with each worn punch after failure. In the case of products formed with Punch 1 (see Fig. 11a), scratches with grooves and ridges parallel to the sliding contact direction were
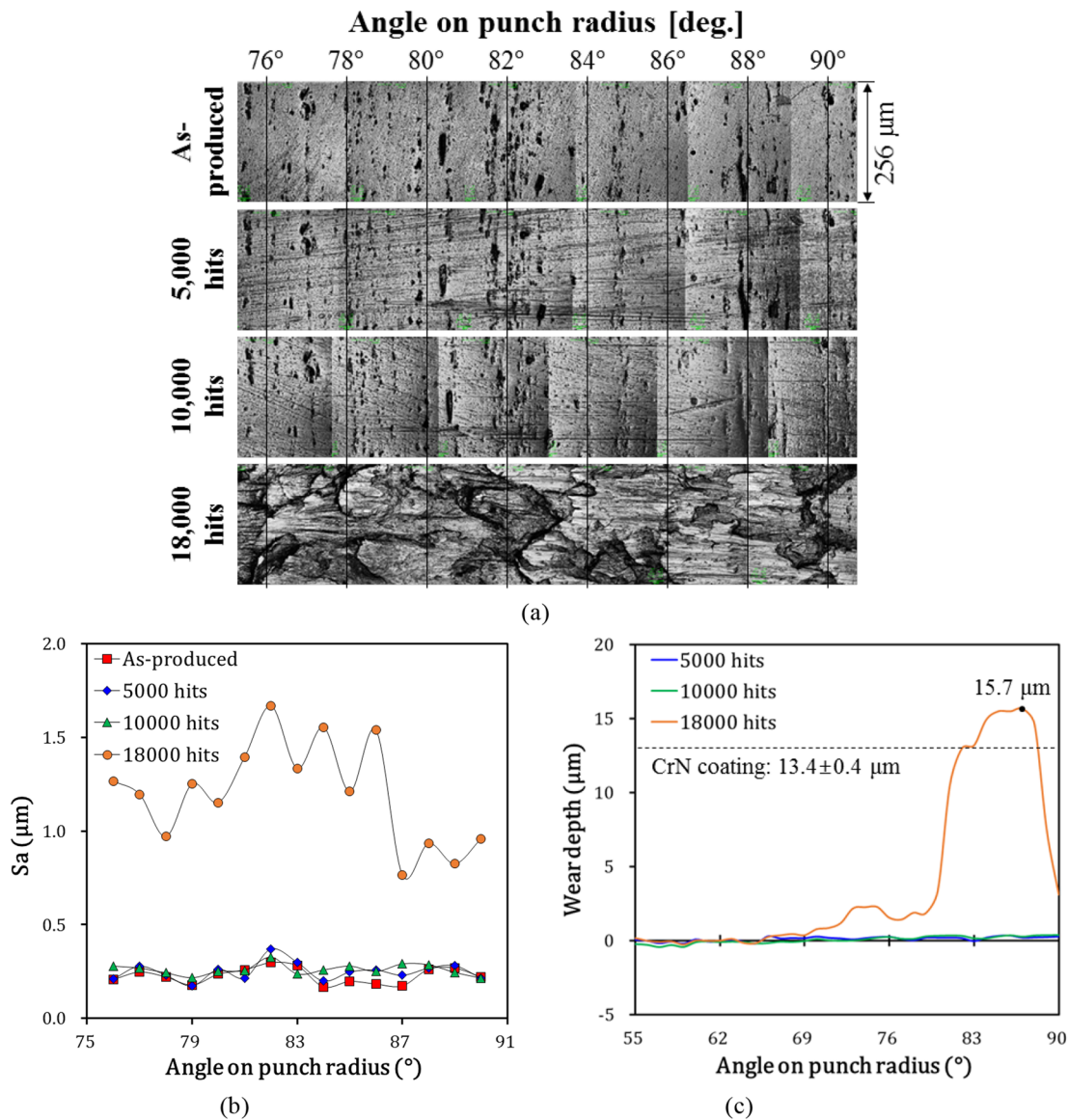
Fig. 7 Surface conditions of Punch 1: **a** surface imaging; **b** surface roughness (Sa); **c** wear depth [22]

observed on the surfaces, with a roughness is 0.732 μm after 17,750 stamping hits. The surface of the product formed at 18,000 stamping hits showed extremely rough states without grooves and ridges, measuring 2.430 μm in roughness. Figure 11b depicts the surface conditions of the product formed with Punch 2. The product surface formed at 58,750 stamping hits also showed scratches with grooves and ridges parallel to the sliding contact direction, with a roughness of 1.013 μm. At 59,000 stamping hits, the surface of the formed product was extremely rough, with a roughness of 1.983 μm. The difference in these product surface qualities is associated with the surface state of the worn punch used for forming. Figure 12 represents the 3D structures of Punch 1 after 17,750 and 18,000 stamping hits, and illustrates the

surface profiles at 32, 64, and 96 μm from the width coordinates of the 3D structures, to assess the wear state on the worn surface. As shown in Fig. 12a, for the surface of Punch 1 observed after 17,750 stamping hits, surface profile within the range of 80 to 128 μm in length was smooth. Within the range of 0 to 80 μm in length, a relatively smooth wear scar was observed, with a wear depth of approximately 5 μm, and the CrN coating layer (13.4 ± 0.4 μm) was not completely worn off. Conversely, as illustrated in Fig. 12b, the wear scar of Punch 1 observed after 18,000 stamping hits was extremely rough within the 0 to 96 μm in length. The wear depth was considered to be deeper than the CrN coating layer (13.4 ± 0.4 μm), and the maximum wear depth of Punch 1, as measured by Bang et al. [25], was 15.7 μm, exceeding
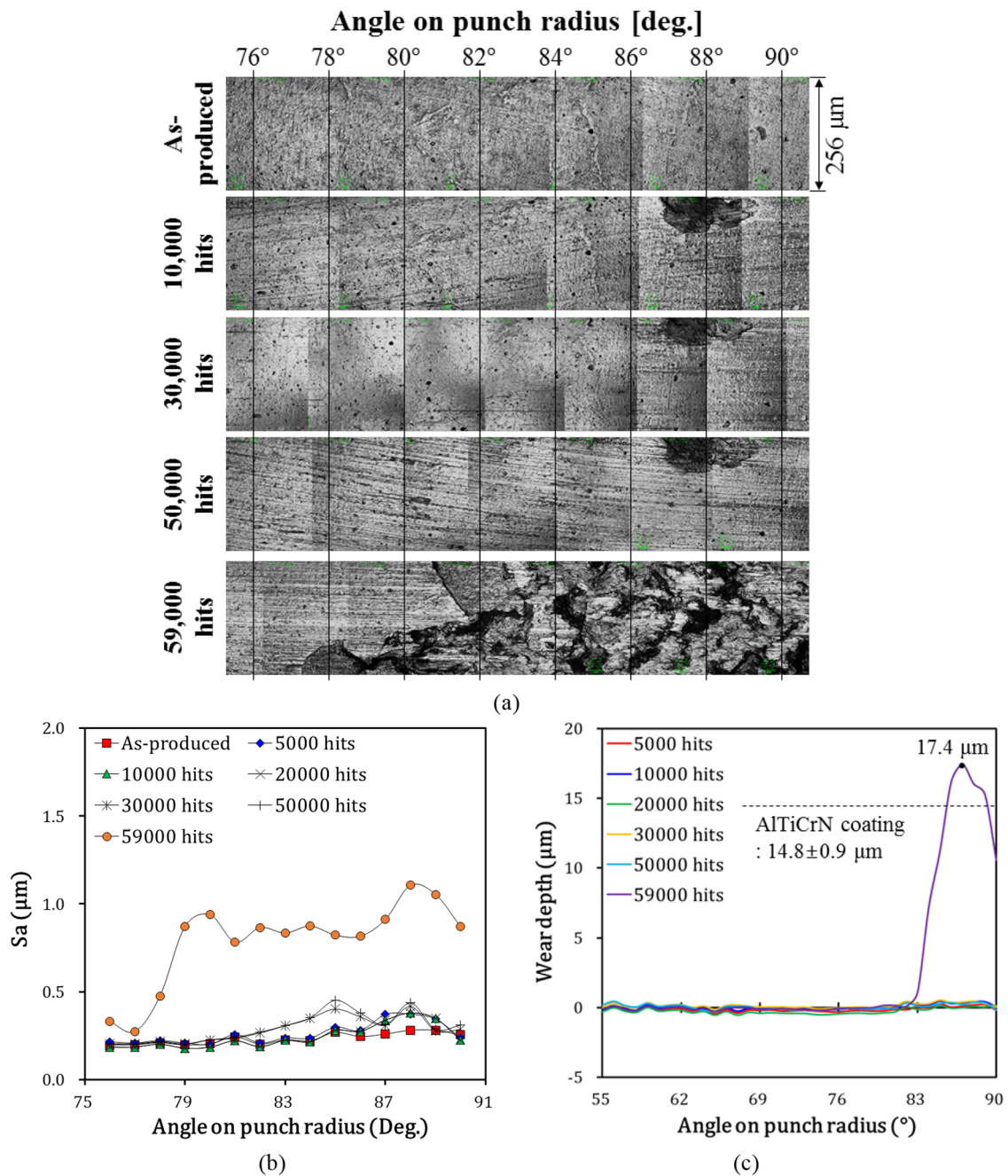
Fig. 8 Surface conditions of Punch 2 [22]: **a** surface imaging; **b** surface roughness (Sa); **c** wear depth

the CrN coating thickness (13.4 ± 0.4 μm). Therefore, PVD CrN coating layers, which do not completely come off, plow the product surface due to the significantly higher hardness of the CrN coatings (2105.9 ± 15.5 $HV_{0.08}$) compared to the TRIP1180 steel sheet (373.2 ± 7.1 $HV_{0.1}$). Furthermore, the extremely rough product surface indicates that the CrN coating layers of Punch 1 are completely peeled off, and the D2 tool steel (788.5 ± 12.2 $HV_{0.1}$) is in direct contact with the sheet metal during the forming process.

The deterioration of the product surface quality was confirmed when the severe wear track suddenly occurred on the punch radius. During the forming process, the punch comes into sliding contact with the steel sheets as the punch stroke progresses. With each stamping hit, the punch radius experiences contact pressure and sliding distance, as depicted in Fig. 6a. Consequently, during continuous wear tests, PVD coated-punches accumulate tangential stress on the punch radius due to repeated sliding contact. These contact
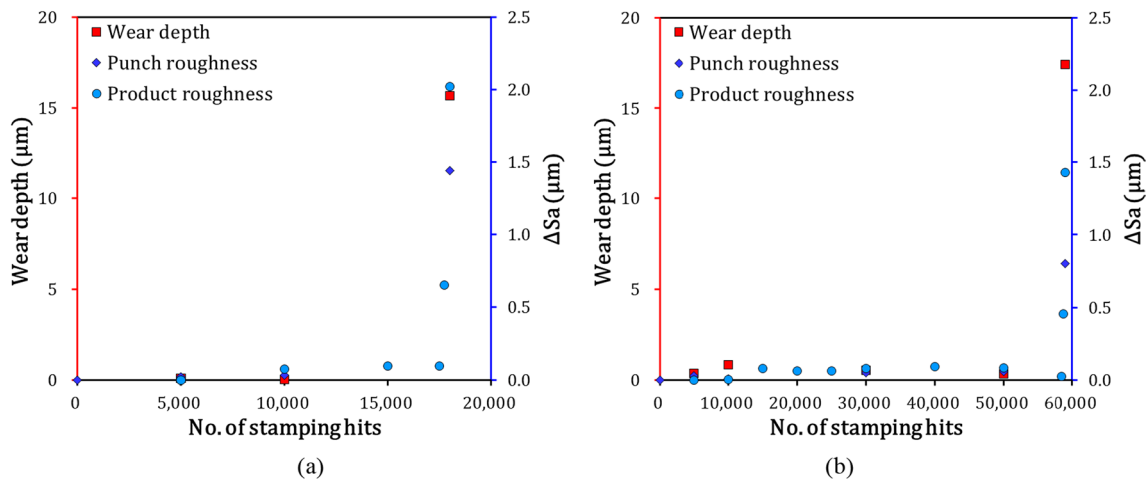
Fig. 9 Correlation between punch surface condition and product surface quality in relation to stamping hits: **a** Punch 1; **b** Punch 2
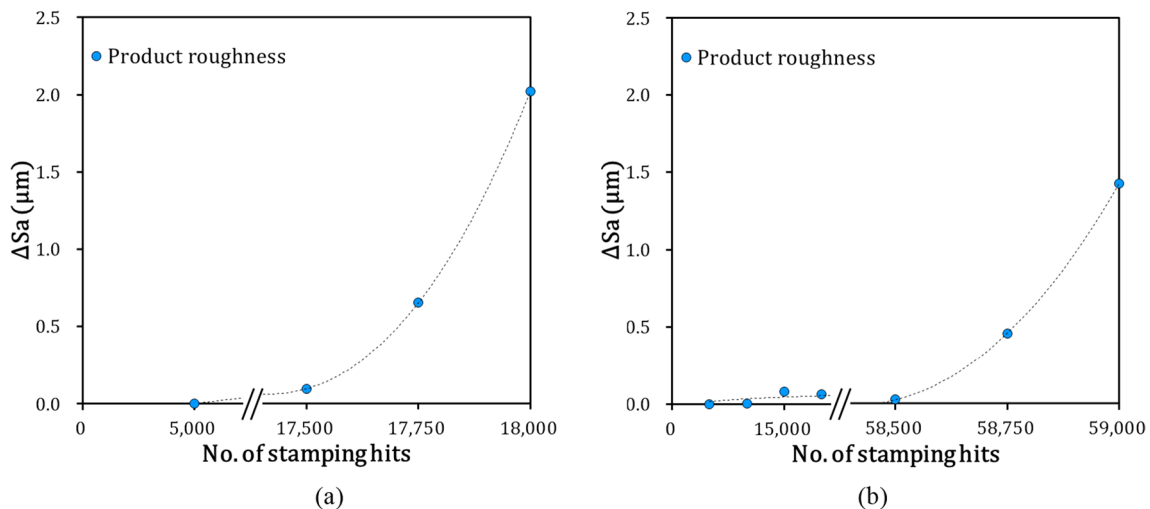
Fig. 10 Product roughness change in relation to stamping hits formed by: **a** Punch 1, and **b** Punch 2

conditions in the sheet metal forming process have similarities to repetitive fretting contacts, and Bang et al. [25] reported that wear of the PVD coating tool in the forming process of the TRIP1180 steel sheet was caused by fretting wear. Fretting refers to wear caused by the cyclic tangential movement of small amplitude at the contact interface under applied load, and the surface damage in fretting regions is approximately proportional to the normal load and slip amplitude. These tangential cycling loads subject the friction surfaces to alternating compression-tension stress, resulting in fretting wear [29]. Voevodin et al. [30] provided evidence that the crack initiation is induced by cyclic tangential

loading during repetitive fretting contacts. Xu et al. [31] observed the evolution of fretting wear due to tangential cycling loads on MoS_2 coating. They found that some micro cracks on the coating surface were initiated at 10^5 cycles, and further propagated at 1.4×10^5 cycles. At 2×10^5 cycles, particle detachment resulted in significant loss of MoS_2 coating protection against fretting wear. Tricoteaux et al. [32] examined the fretting wear scars generated by repeated fretting contact on CrN coating. They observed the initiation and propagation of micro cracks on the CrN coating due to the repeated cyclic tangential loads, which eventually

After 17,750 hits

After 18,000 hits

After 58,750 hits

After 59,000 hits

(a)

(b)
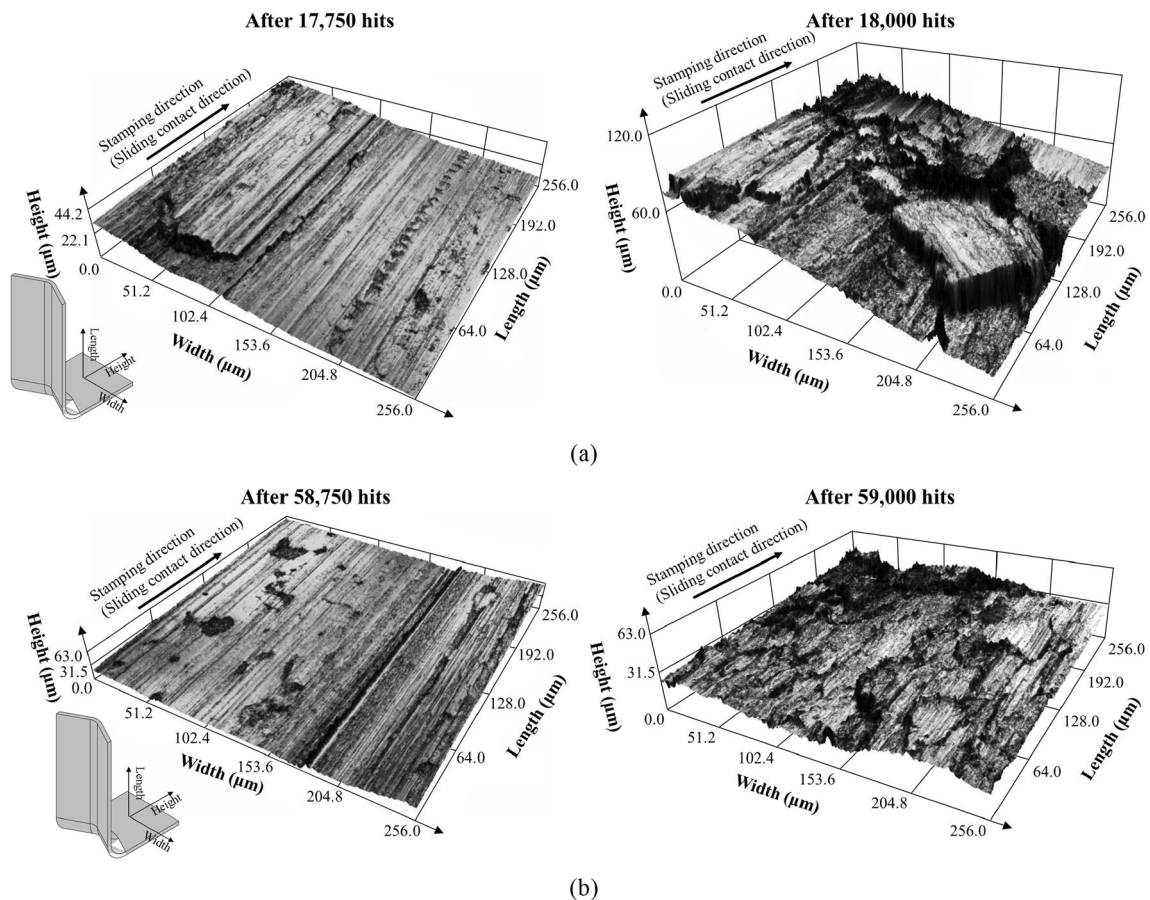
Fig. 11 3D surface profiles of of the products formed with worn punches: **a** Punch 1; **b** Punch 2

merged and peeled off. To examine the wear scars on CrN-coated Punch 1 in the forming process of TRIP1180 steel sheet, the surface of Punch 1 was inspected using the CLSM with a 100× objective lens (see Fig. 13). Figure 13a shows cracks at the edge of the wear scar caused by repetitive sliding contact during the forming process. Figure 13b shows delamination of cracks on the CrN coating layers due to crack propagation and coalescence resulting from repeated tangential loading. Therefore, microscopic analysis confirms that the wear mechanism of CrN coated tools in the forming of TRIP1180 steel sheets is due to fretting wear.

4 Conclusions

A wear test was conducted using a newly designed progressive die for the forming of TRIP1180 sheet. In the tests, two different coatings, PVD CrN and AlTiCrN, were applied to bending punches. To identify the evolutionary behavior of the workpiece surface quality, sheet samples were taken at

regular interval of 250 stamping hits. The effect of tool wear condition on the surface quality was presented by examining the correlation among tool wear depth, tool roughness, and product roughness according to the number of stamping hits. The main conclusions of the present work can be summarized as follows.

(1) The experiment showed that micro scratches on the punch surface had little effect on the change of the wear depth when measured before failure, and the product surface roughness was comparable to the roughness of the as-received sheet.

(2) Once the tool wear was initiated by the fretting wear mechanism, the tool surface condition directly affected the deterioration of the product surface quality. Also, the tools subjected to repeated tangential loads during stamping process could induce the micro cracks, which led to wear with magnitudes smaller than the thickness of coating layer.

(3) When sheets were formed with the punch with partially peeled-off coatings, the product surface roughness was very small (less than 1.0 μm) with grooves

(a)

(b)
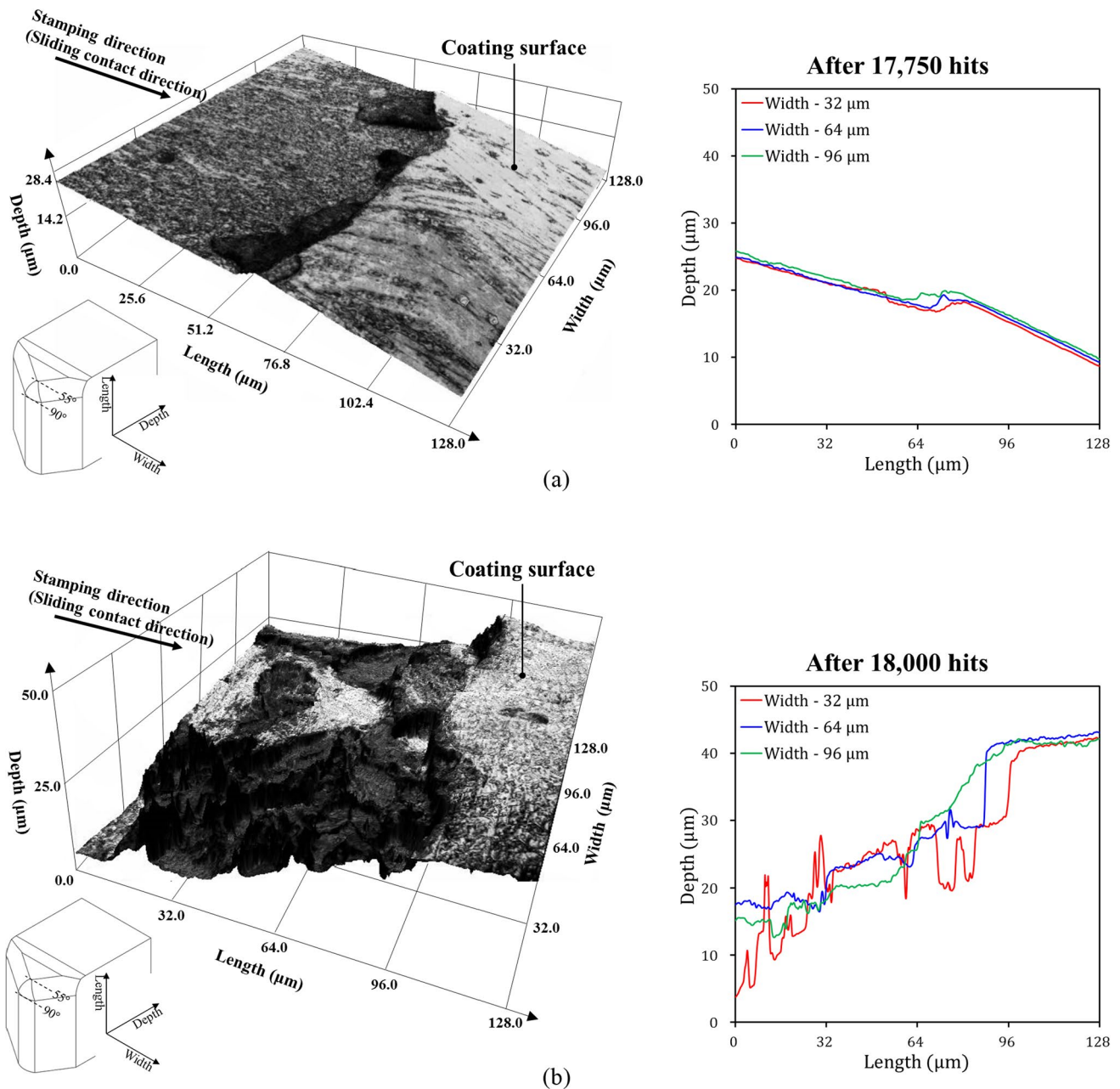
Fig. 12 3D surface profiles of worn surface on Punch 1 and their surface profiles along length direction at the width of 32, 64, and 96 μm: **a** after 17,750 stamping hits; **b** after 18,000 stamping hits [22]

and ridges. After short stamping duration, tool wear increases exponentially, which eventually caused complete delamination of the coating layers.

(4) The extremely rough product surface without grooves and ridges resulted from punch contacts with completely damaged coating layers during the forming process.

(5) It was found that the surface quality of sheet product could be accurately correlated with the wear state and surface condition of the tool. This study suggests that

the evolution of tool wear behaviors can be efficiently predicted by investigating of the product surface quality.

(a)

(b)
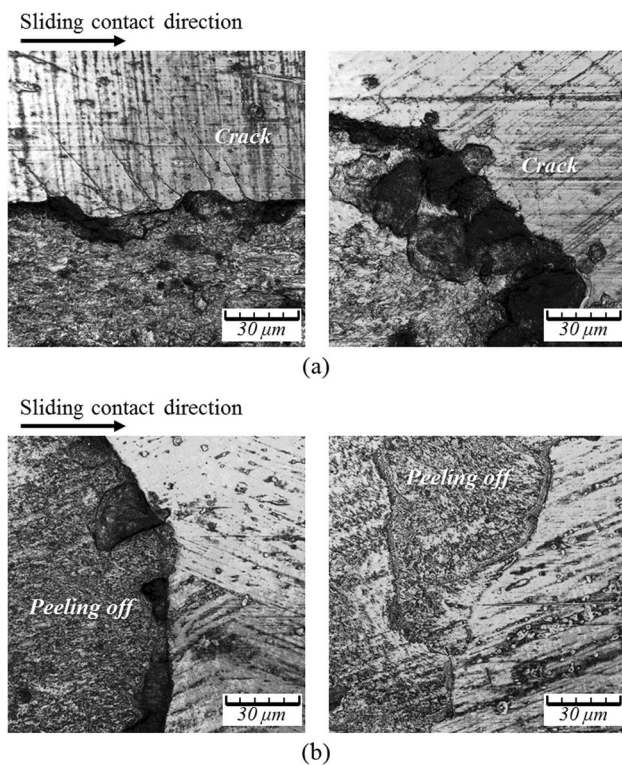
Fig. 13 Cracks and delamination of coating layers on wear scar of CrN coated tool (Punch 1): **a** Cracks on fretting wear scar; **b** delamination of CrN coating layers after repeated tangential loading

Declarations

Competing interests The authors declare that they have no known competing financial interests or personal relationships that could have appeared to influence the work reported in this paper. The authors declare the following financial interests/personal relationships which may be considered as potential competing interests:

References

1. A. Jambor, M. Beyer, Mater. Design **18**, 203 (1997). https://doi.org/10.1016/S0261-3069(97)00049-6

2. S.S. Cheon, D.G. Lee, K.S. Jeong, Compos. Struct. **38**, 229 (1997). https://doi.org/10.1016/S0263-8223(97)00058-5

3. A.I. Taub, A.A. Luo, MRS Bull. **40**, 1045 (2015). https://doi.org/10.1557/mrs.2015.268

4. X. Sun, F. Meng, J. Liu, J. McKechnie, J. Yang, J. Clean. Product. **220**, 1 (2019). https://doi.org/10.1016/j.jclepro.2019.01.225

5. H. Safari, H. Nahvi, M. Esfahanian, Int. J. Crashworthiness **23**, 645 (2018). https://doi.org/10.1080/13588265.2017.1389624

6. C. Lesch, N. Kwiaton, F.B. Klose, Steel Res. Int. **88**, 1700210 (2017). https://doi.org/10.1002/srin.201700210

7. B. Podgornik, S. Hogmark, O. Sandberg, Surf. Coat. Tech. **184**, 338 (2004). https://doi.org/10.1016/j.surfcoat.2003.11.002

8. M.P. Pereira, W. Yan, B.F. Rolfe, Wear **274**, 355 (2012). https://doi.org/10.1016/j.wear.2011.10.006

9. X. Luo, H. Duan, J. Li, S. Zhan, D. Jia, J. Tu, Y. Li, Y. Chen, Met. Mater. Int. **28**, 988 (2022). https://doi.org/10.1007/s12540-020-00937-w

10. B. Podgornik, S. Hogmark, J. Mater. Process. Technol. **174**, 334 (2006). https://doi.org/10.1016/j.jmatprotec.2006.01.016

11. B. Podgornik, J. Vižintin, S. Hogmark, Surf. Eng. **22**, 235 (2006). https://doi.org/10.1179/174329406X122946

12. B. Podgornik, J. Jerina, Surf. Coat. Technol. **206**, 2792 (2012). https://doi.org/10.1016/j.surfcoat.2011.11.041

13. Y. Hou, W. Zhang, Z. Yu, S. Li, Int. J. Adv. Manuf. Technol. **43**, 1010 (2009). https://doi.org/10.1007/s00170-008-1780-2

14. A. Ghiotti, S. Bruschi, Wear **271**, 2454 (2011). https://doi.org/10.1016/j.wear.2010.12.043

15. ÖN. Cora, K. Namiki, M. Koç, Wear **267**, 1123 (2009). https://doi.org/10.1016/j.wear.2008.12.111

16. E. Büyükkayacı, İ Şimşek, D. Özyürek, Met. Mater. Int. **27**, 4618 (2021). https://doi.org/10.1007/s12540-020-00711-y

17. H. Sıralı, D. Şimşek, D. Özyürek, Met. Mater. Int. **27**, 4110 (2021). https://doi.org/10.1007/s12540-020-00735-4

18. O. Ogunbiyi, T. Jamiru, R. Sadiku, O. Adesina, O.S. Adesina, B.A. Obadele, Met. Mater. Int. **28**, 695 (2022). https://doi.org/10.1007/s12540-020-00871-x

19. P. Groche, M. Christiany, Wear **302**, 1279 (2013). https://doi.org/10.1016/j.wear.2013.01.001

20. A. Gonzalez-Pociño, F. Alvarez-Antolin, J. Asensio-Lozano, Materials **12**, 2831 (2019). https://doi.org/10.3390/ma12172831

21. R.G. Woodward, A. Toumpis, A. Galloway, Wear **496**, 204283 (2022). https://doi.org/10.1016/j.wear.2022.204283

22. Y.E. Jeong, D.S. Shim, Met. Mater. Int. **28**, 2621 (2022). https://doi.org/10.1007/s12540-021-01156-7

23. N. Jeyaprakash, C.H. Yang, G. Prabu, R. Clinktan, Met. Mater. Int. **28**, 2997 (2022). https://doi.org/10.1007/s12540-022-01198-5

24. J. Bang, N. Park, J. Song, H.G. Kim, G. Bae, M.G. Lee, Metals **11**, 306 (2021). https://doi.org/10.3390/met11020306

25. J. Bang, M. Kim, G. Bae, J. Song, H.G. Kim, M.G. Lee, Met. Mater. Int. **29**, 327 (2023). https://doi.org/10.1007/s12540-022-01244-2

26. M.P. Pereira, W. Yan, B.F. Rolfe, Wear **265**, 1687 (2008). https://doi.org/10.1016/j.wear.2008.04.042

27. M.P. Pereira, W. Yan, B.F. Rolfe, Wear **268**, 1275 (2010). https://doi.org/10.1016/j.wear.2010.01.020

28. J. Bang, M. Kim, G. Bae, H.G. Kim, M.G. Lee, J. Song, Materials **15**, 4509 (2022). https://doi.org/10.3390/ma15134509

29. R.B. Waterhouse, Int. Mater. Reviews **37**, 77 (1992). https://doi.org/10.1179/imr.1992.37.1.77

30. M. Lin, A. Nemcova, A.A. Voevodin, A. Korenyi-Both, T.W. Liskiewicz, N. Laugel, A. Matthews, A. Yerokhin, Tribo. Int. **154**, 106723 (2021). https://doi.org/10.1016/j.triboint.2020.106723

31. J. Xu, M.H. Zhu, Z.R. Zhou, Ph. Kapsa, L. Vincent, Wear **255**, 253 (2003). https://doi.org/10.1016/S0043-1648(03)00053-X

32. A. Tricoteaux, P.Y. Jouan, J.D. Guerin, J. Martinez, A. Djouadi, Surf. Coat. Technol. **174–175**, 440 (2003). https://doi.org/10.1016/S0257-8972(03)00597-8

Publisher's Note Springer Nature remains neutral with regard to jurisdictional claims in published maps and institutional affiliations.